P-77: High Efficiency Polymer-Based Electrophosphorescent Organic Light-Emitting Diode

Zhiliang Xie, Chengfeng Qiu, Haiying Chen, Benzhong Tang, Man Wong, Hoi-Sing Kwok

Center for Display Research, Hong Kong University of Science and Technology

Clear Water Bay, Kowloon, Hong Kong

Abstract

We investigate the characteristics of an organic light-emitting diode with phosphorescent polymer. Two types of double layer diodes based on poly(9-vinylcarbazole) (PVK) doped with phosphorescent fac tris(2-phenylpyridine) iridium (III) [Ir(ppy)$_3$] /aluminum (III) bis(2-methyl-8-quinolinato) 4-phenylphenolate (BAlq) and [PVK doped Ir(ppy)$_3$]/Alq$_3$ have been investigated. It is found that BAlq can serve as an electron transport layer as well as a hole blocking layer. At the optimal dopant concentration, a high efficiency OLED can be obtained. At 2wt% Ir(ppy)$_3$, an effective external quantum efficiency of 10% photons/electron, a low turn-on voltage of 6V and a luminance power efficiency of 7.3L/W can be achieved.

1. Introduction

Recently, nearly 100% [1-3] internal emission quantum efficiency has been obtained by harvesting both singlet and triplet excitons in organic light-emitting diodes (OLEDs) doped with phosphorescent emitters containing heavy metals. The strong spin-orbit coupling of a heavy metal enhances inter-system crossing and mixes the single and triplet states. Effective external quantum efficiency (h_{EQE}) of 19% photons/electron and luminance power efficiency (h_P) of 70 *L/W* have been demonstrated in small molecule OLEDs [2,3].

Phosphorescent dopants have also been applied to OLEDs based on polymers [4-14]. An important advantage of polymer-based OLEDs over their small-molecule counterparts is their compatibility with solution processing. This potentially allows a lower cost of production using room temperature spin-coating, screen printing or ink-jet printing techniques.

Using a single 100-200nm thick blend of hole-transporting poly(9-vinylcarbazole) (PVK) and an electron-transporting 2-(4-biphenyl)-5-(4-tert-butylphenyl)-1,3,4-oxadiazole doped with tris[9,9-dihexyl-2-(pyridinyl-2') fluorene] iridium (III), Gong et al [12] demonstrated a high h_{EQE} of 10% photons/electron at an optimal doping concentration of 0.3wt%. However, the reported turn-on voltage was relatively high, resulting in a low h_P of only 2.5 *L/W*. Using a double-layer structure of fac tris(2-phenylpyridine) iridium(III) - Ir(ppy)$_3$ - doped PVK as the hole-transport layer and 1,3-bis[(4-tert-butylphenyl)-1,3,4-oxadiazolyl] phenylene as the electron-transport layer, Yang et al [13] reported a higher h_P of 5.8 *L/W* but a lower h_{EQE} of 7.5% photons/electron at a doping concentration of 6.8wt%. Adding a hole-blocking

layer, Vaeth et al [14] recently reported a high h_{EQE} of 8.5% in a relatively more complex triple-layer device.

Since the performance of an OLED is sensitive to both the arrangement and the choice of the constituent organic layers, further improvement is quite possible. In this paper, double-layer diodes were constructed as shown in Fig. 1. Two types of devices were made. The difference is that aluminum (III) bis(2-methyl-8-quinolinato) 4-phenylphenolate (BAlq) instead of Alq$_3$ is used in the Type B device. It was found in Type B device that BAlq can serve as a hole blocking layer as well as an electronic transport layer. Type B device therefore has a much better performance than Type A device. When the concentration of Ir(ppy)$_3$ reaches its optimal value in Tape B device, a high h_P of 7.3 *L/W* and a high h_{EQE} of 10% can be obtained.
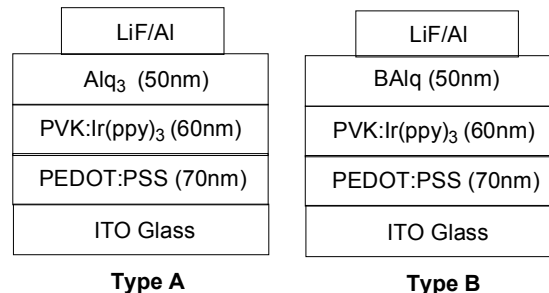

Fig. 1. The structures of EL devices.

2. Experimental

Glass coated with 70nm, 30 $\Omega/\square$ indium-tin oxide (ITO) was used as the starting substrate. The sequence of pre-cleaning prior to the deposition of the organic layers consisted of a 50°C ultrasonic detergent soak for 30min, de-ionized water spray for 10min, ultrasonic de-ionized water soak for 30min, 110°C oven bake dry for 1-2hr and ultra-violet/ozone illumination for 10min. Sequential spin-coatings of 60nm poly(ethylene dioxythiophene): poly(styrene sulfonic acid) (PEDOT:PSS) and 50nm Ir(ppy)$_3$ doped PVK at room temperature under ambient conditions were followed by 54°C vacuum oven solvent evaporation and bake dry for 2hr. Subsequently, 50nm BAlq (for device Type B) or Alq$_3$ (for device Type A) were deposited by thermal vacuum evaporation in a chamber with a base pressure of 1 μTorr. The cathode, consisting of 1nm lithium fluoride (LiF) and 150nm aluminum (Al) [15], was subsequently evaporated through a

shadow mask. The layer thickness during evaporation was measured in situ using a quartz crystal monitor. A Tencor P-10 Surface Profiler was used to determine the thickness of the spin-coated films.

Electro-luminescence (EL) photometric characteristics were measured using a Kollmorgen Instrument PR650 photo-spectrometer. Current-voltage characteristics were measured using a Hewlett-Packard HP4145B Semiconductor Parameter Analyzer.

3.   Results and discussions

Excited using the 337nm line of a He-Cd laser, the normalized photo-luminescence (PL) spectra of pure $Ir(ppy)_3$, PVK doped with various concentrations of $Ir(ppy)_3$ and pure PVK are shown in Fig. 2(a). PL peaks are observed at ~400nm for PVK singlet emission and at ~516nm for $Ir(ppy)_3$ triplet emission (Fig. 2(b)). Below a critical $Ir(ppy)_3$ concentrations of 10wt%, the Förster transfer of excitons is incomplete because of the larger average separation between an excited site on the PVK host and an $Ir(ppy)_3$ dopant. Therefore an emission near ~400nm attributed to the PVK host is observed. The separation reduces and the exciton transfer efficiency and improves with increasing concentration of $Ir(ppy)_3$, leading to almost complete disappearance of the emission near 400nm at $Ir(ppy)_3$ concentrations above 10wt%.
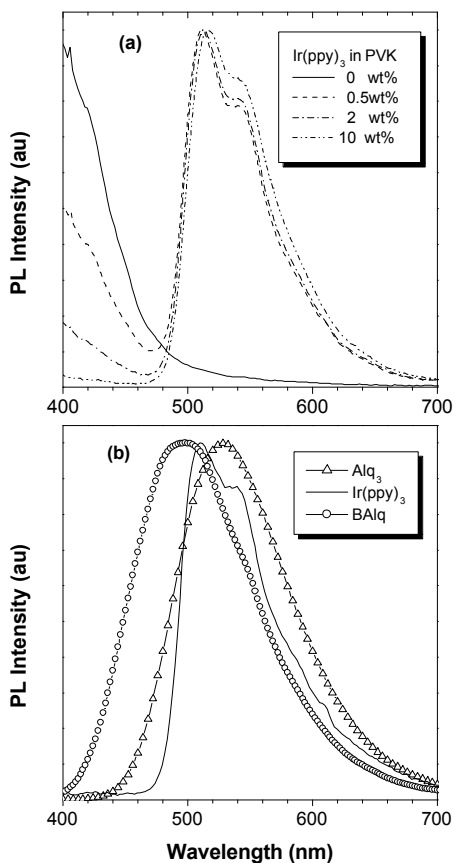
The PL spectra of Alq_3, BAlq, and $Ir(ppy)_3$ are shown in Figs. 2(b). The emissions of Alq_3 and BAlq peak at ~530 and ~480 nm, respectively, which are clearly deferent from that (~516 nm) of $Ir(ppy)_3$.

The EL spectra of Type A and Type B devices are shown in Figs. 3(a) and 3(b). Unlike the PL spectra, the most distinguishing feature of the EL spectra both devices Type A and Type B are the absence of any PVK-induced emission near ~400nm, irrespective of the $Ir(ppy)_3$ concentration. The absence of major PVK related emission features implies a charge trapping rather than an exciton transfer mechanism [16, 17]. In Fig. 3(a), all EL spectra are quite similar with the different doping concentration. The EL spectra have two peak, one is near ~516nm contribution of $Ir(ppy)_3$ emission and the other is ~545nm contribution of Alq_3 emission, referencing to the PL spectrum of Alq_3 (Fig.2(b)). The intensity of the EL from of $Ir(ppy)_3$ and Alq_3 are same, and almost unchanged with the doping concentration. In Fig. 3(b), the EL spectra for device Type B is dominated by $Ir(ppy)_3$-induced peaks near ~516nm. The spectra show the appearance of a blue emission shoulder at ~460nm with $Ir(ppy)_3$ concentration below 2wt%. It can be inferred by comparing with the BAlq PL spectrum (Fig. 2(b)) that this blue emission originated from BAlq. The blue emission disappeared above 2wt%.

Fig. 2. (a) PL spectra of PVK doped with various concentrations of $Ir(ppy)_3$. (b) PL spectra of Alq_3, BAlq and $Ir(ppy)_3$.
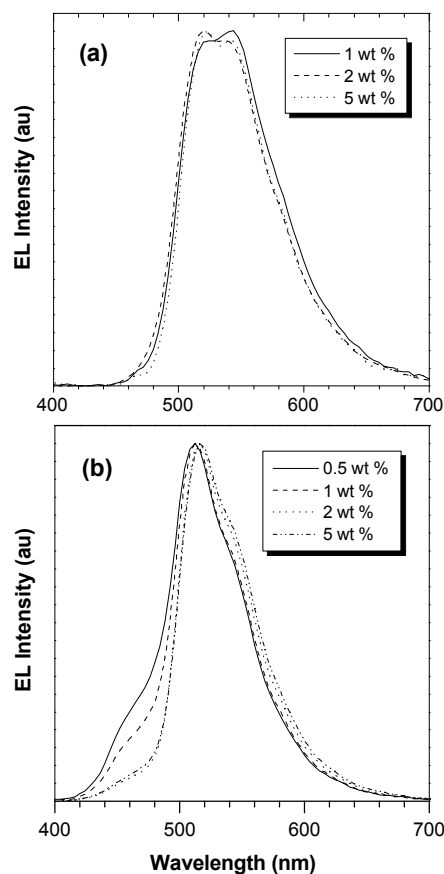

Fig. 3. (a) EL Spectra of the device Type A with various doping concentration. (b) EL Spectra of the device Type B with various doping concentration.

The Luminance – Current density – Voltage (*L-J-V*) characteristics of Type A and Type B diodes are shown in Figs. 4(a) and 4(b), respectively. It can be seen from Fig. 4(a) that both (*L-J*) and (*V-J*) corves show little change with the variation of the doping concentration. The brightness are almost same at the given current density regardless the doping concentration. For Type B diode (Fig. 4(b)), similar trends are observed on the (*V-J*) characteristics. However, the (*L-J*) characteristics show large dependence on the doping concentration. At the given current density, the brightness increases with increasing $Ir(ppy)_3$ concentration from 0.5 to 2wt%. Further increasing the concentration results in a decrease in brightness.
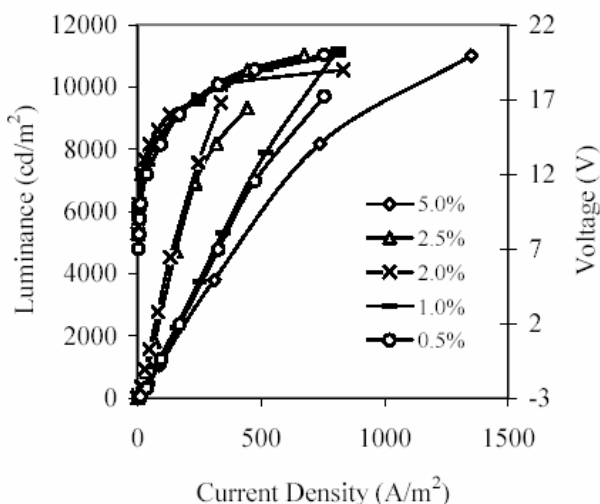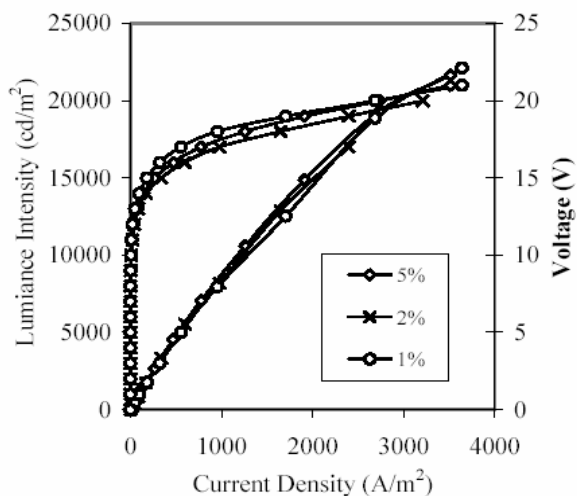

Fig. 4. (a) Luminance (*L*)-current density (*J*) − voltage (*V*) characteristics of the device Type A with various doping concentrations. (b) *L*-*J*–*V* characteristic of the device Type B with various doping concentrations.
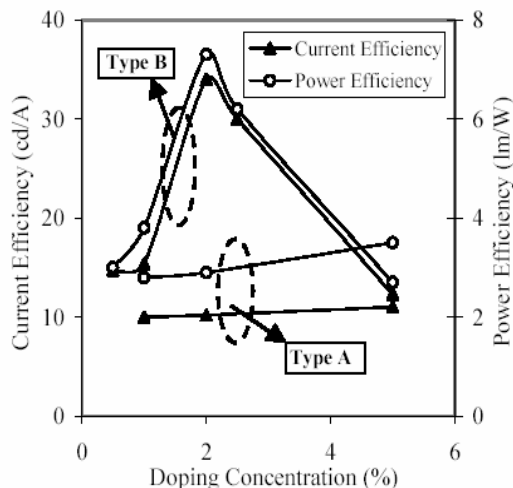

Fig. 5 Dependence of the current efficiency and power efficiency on $Ir(ppy)_3$ concentration of devices Type A and Type B.

The dependences of both peak current efficiency (h) and h_P on $Ir(ppy)_3$ concentration are shown in Fig. 5. Both efficiencies of Type A diodes show little increase with increasing the $Ir(ppy)_3$ concentration. For Type B, the efficiencies of both types of diodes first increase and then decrease with increasing the $Ir(ppy)_3$ concentration. A peak h of 34 cd/A and h_P of 7.4 *L/W* can be obtained at ~2wt%. The corresponding h_{EQE} is 10%. Beyond this optimal concentration, the emission efficiency decreases due to aggregate quenching [12].

Clearly, the EL efficiencies can be dramatically enhanced by using BAlq (type A) instead of Alq_3 (type B). The reason maybe closely related to the difference between the HOMO levels of BAlq and Alq_3. Further experiments and analyses are being done.

4. Conclusion
The performance of OLEDs fabricated with $Ir(ppy)_3$ doped PVK and BAlq or Alq_3 respective as the hole- and electron-transport layers has been studied. It is found that BAlq functions additionally as a hole-blocking layer, resulting a great improvement in EL efficiency. The peak efficiency of the diode is sensitive to the concentration of $Ir(ppy)_3$. At 2wt% concentration, a peak current efficiency of 34-cd/A and a peak power efficiency of 7.3 *L/W* have been achieved.

5. Acknowledgements

6. References
[1] C. Adachi, M. A. Baldo, S. R. Forrest, and M. E. Thompson, Appl. Phys. Lett. **77**, 904 (2000).

[2] C. Adachi, M. A. Baldo, M. E. Thompson, and S. R. Forrest, J. Appl. Phys. **90**, 5048 (2001).

[3] M. Ikai, S. Tokito, Y. Sakamoto, T. Suzuki, and Y. Taga, Appl. Phys. Lett. **79**, 156 (2001)

[4] R. H. Friend, R. W. Gymer, A. B. Holmes, J. H. Burroughes, R. N. Marks, C. Taliani, D. D. C. Bradley, D. A. Dos Santos, J. L. Bredas, M. Logdlund, and W. R. Salaneck, Nature (London) **397**, 121 (1999).

[5] C. L. Lee, K. B. Lee, and J. J. Kim, Appl. Phys. Lett. **77**, 2280 (2000).

[6] T. F. Guo, S. C. Chang, Y. Yang, R. Kwong, and M. E. Thompson, Org. Electron. **1**, 15 (2001).

[7] D. F. O'Brien, C. Giebler, R. B. Fletcher, J. Cadlby, L. C. Palilis, D. G. Lidzey, P. A. Lane, D. D. C. Bradley, and W. Blau, Synth. Met. **116**, 379 (2001).

[8] S. Lamansky, R. C. Kwong, M. Nugent, P. I. Djurovich, and M. E. Thompson, Org. Electron. **2**, 53 (2001).

[9] S. Lamansky, P. Djurovich, D. Murphy, F. Abdel-Razzaq, H.-E. Lee, C. Adachi, P. E. Burrows, S. R. Rorrest, and M. E. Thompson, J. Am. Chem. Soc. **123**, 4304 (2001).

[10] W. Zhu, Y. Mo, M. Yuan, W. Yang, and Y. Cao, Appl. Phys. Lett. **80**, 2045 (2002).

[11] F-C. Chen, and Y. Yang, Appl. Phys. Lett. **80**, 2308 (2002).

[12] X. Gong, M. R. Robinson, J. C. Ostrowski, D. Moses, G. C. Bazan, and A. J. Heeger, Adv. Mater. **14**, 581 (2002).

[13] M-J. Yang, and T. Tsutsui, Jpn. J. Appl. Phys. **39**, L828 (2000).

[14] K. M. Vaeth and C. W. Tang, J. Appl. Phys. **92**,3447 (2002)

[15] C.F. Qiu, H. Chen, M. Wong and H. S. Kwok, IEEE Trans. on Electron Devices, **48**, 2131 (2001).

[16] C.F. Qiu, H.Y. Chen, M. Wong and H.S. Kwok, IEEE Trans. on Electron Device, **49**, 1540 (2002).

[17] H. Murata, C.D. Merritt, Z.H. Kafafi, IEEE J. Select. Topics in Quantum Electron., **4**, 119 (1998)